Proc. Natl. Acad. Sci. USA
Vol. 90, pp. 1350–1353, February 1993
Physics

Mechanism of superconductivity in K_3C_{60}

(alkali/Buckminsterfullerene/electron–phonon coupling)

GUANHUA CHEN AND WILLIAM A. GODDARD III

Materials and Molecular Simulation Center, California Institute of Technology, 139-74, Pasadena, CA 91125

Contributed by William A. Goddard III, November 13, 1992

ABSTRACT **Using electronic states and phonon states from the first-principles calculations and including both conventional electron–phonon charge coupling and Jahn–Teller coupling, we predict T_c and other superconducting properties. The only adjustable parameter in the theory is the screening length, R_{sc}. Using R_{sc} = 0.8–1.0 Å, we find excellent agreement with experiment for T_c (16–18 K), pressure dependence of T_c (ΔT_c = −6 to −10 K for 1 GPa), and ^{12}C to ^{13}C isotope shift (α_C = 0.2); experimental values: 19 K, −7 K, and 0.3, respectively.**

A number of superconducting alkali compounds of C_{60} (M_3C_{60}) have been synthesized (1–5), leading to transition temperatures T_c from 2.5 K to 33 K. Several quite different mechanisms (6–12) have been proposed to explain the superconductivity in these materials.

A suggestion by Lannoo *et al.* (6, 7), Johnson *et al.* (8) and Varma *et al.* (9) is that dynamic Jahn–Teller (JT) coupling involving high-frequency intramolecular vibrations strongly scatter electrons near the Fermi surface, leading to superconductivity. On the other hand, Zhang *et al.* (10) estimated various contributions to the electron–electron interaction in K_3C_{60} and argued that the K^+ optical-phonon modes induce a strong attraction that is the main source of superconductivity. In addition to phonon-mediated electron-pairing mechanisms, Chakravarty *et al.* (11) and Baskaran and Tosatti (12) argue that two electrons may pair by electron–electron exchange and correlation on a single C_{60} molecule.

Hamiltonian and Electron–Phonon Couplings

We present here a first-principles, quantitative study of the superconductivity K_3C_{60}, using the Hamiltonian equation

$$H = H_{ph} + H_e + H_{ee} + H^Q_{eph} + H^{JT}_{eph}, \quad [1]$$

where each term is defined below.

Phonon States (H_{ph}). We started with the graphite force field (GraFF) developed by Guo *et al.* (13) for describing the structure, elastic constants, and phonons of graphite and intercalated graphite. Without adjustments, the GraFF leads to an excellent description of the vibrational levels of C_{60} (4% average absolute error for A_g and H_g). The lattice constants of K_3C_{60} are within 0.1 Å of experiment (14, 15), and the predicted linear compressibilities (13) of K_3C_{60}, β = 1.13 × 10^{-3} kbar^{-1}, is close to experiment (15), 1.20(9) × 10^{-3} kbar^{-1}.

Using the predicted structure of fcc K_3C_{60} [a = 14.18 Å, experimental (14, 15) a = 14.24 Å], we calculated the 189 phonon modes (eigenvectors and frequencies) for each point of a 6 × 6 × 6 grid in the Brillouin zone. These modes partition into 174 high-frequency intramolecular bands (260–1520 cm^{-1}) plus six lattice modes (130–140 cm^{-1}) involving tetrahedral K, three lattice modes (20–50 cm^{-1}) involving octahedral K, three C_{60} librational modes (30–40 cm^{-1}), and three acoustic phonon modes. We write H_{ph} as

$$H_{ph} = \sum_{k,j} \Omega_{kj}\, a^+_{kj} a_{kj}, \quad [2]$$

where Ω_{kj} is the frequency of mode j (j = 1189) with momentum $\mathbf{k}$.

Electronic States (H_e). For H_e we fitted the local density approximation (LDA) description of the conduction band by Erwin and Pickett (16) to a tight-binding Hamiltonian

$$H_e = \sum_{i,j}^{nn} t^{(1)}_{ij} c^+_{mi} c_{nj} + \sum_{k}^{nnn} t^{(2)}_{k} c^+_{mk} c_{lk}, \quad [3]$$

with the nearest (*nn*) and the next-nearest neighbor (*nnn*) hopping matrix elements. This leads to a density of states of $N(0)$ = 11.5 [the units of $N(0)$ are states per eV per C_{60}] and a Fermi energy of E_f = 0.23 eV. These compare well with the LDA results (16) of $N(0)$ = 13.2 and E_f = 0.26 eV.

We determined the Fermi surface by calculating the states from H_e at 1,000,000 points in the Brillouin zone, evaluating the Fermi energy, and selecting 330 points within 0.001 eV of the Fermi energy.

Dynamic Charge Coupling (H^Q_{eph}). Dynamic charge coupling describes the changes in the electron–ion coulomb interactions, due to vibrations (for fixed electronic orbitals). We calculated the electron–phonon coupling matrix $M_{\mathbf{k}'\mathbf{k}j}$, using the exact phonon eigenvectors and eigenenergies with a local Wannier orbital representation for the conduction electrons.

The charge-coupling Hamiltonian is written as

$$H^Q_{eph} = \sum_l \sum_{n\alpha} \Delta\mathbf{R}_{n\alpha} \cdot \nabla_{n\alpha} V_{ei}(\mathbf{r}_l - \mathbf{R}^{(0)}_{n\alpha}), \quad [4]$$

where $V_{ei}(r) = \exp(-r/R_{sc})/r$ is the screened electron–ion coulomb interaction with screening length R_{sc}, $\mathbf{R}^{(0)}_{n\alpha}$ is the equilibrium position of the αth ion in the nth unit cell, and $\Delta\mathbf{R}_{n\alpha}$ is its displacement,

$$\Delta\mathbf{R}_{n\alpha} = \sum_{\mathbf{k}j} \sqrt{1/NM_\alpha}\, Q(\mathbf{k}j)\xi(\alpha|\mathbf{k}j)\exp(i\mathbf{k}\cdot\mathbf{R}^{(0)}_{n\alpha}), \quad [5]$$

where $\xi(\alpha|\mathbf{k}j)$ is the phonon eigenvector of momentum $\mathbf{k}$ and mode j and $Q(\mathbf{k}j)$ is its amplitude.

Using the tight-binding picture, H^Q_{eph} simplifies to

$$H^Q_{eph} = \frac{1}{V^{1/2}} \sum_{\mathbf{k}'\mathbf{k}j} M_{\mathbf{k}'\mathbf{k}j} c^+_{\mathbf{k}'} c_{\mathbf{k}} (a^+_{-\mathbf{q}j} + a_{\mathbf{q}j}) \quad [6]$$

$$M_{\mathbf{k}'\mathbf{k}j} = -i \sum_{\mathbf{G},\alpha} \left(\frac{\hbar}{2\rho_\alpha \Omega_{\mathbf{q}j}}\right)^{1/2} e^{-i\mathbf{G}\cdot\mathbf{R}_\alpha} \hat{V}_{ei}(\mathbf{q}+\mathbf{G})\xi(\alpha|\mathbf{q}j) \cdot(\mathbf{q}+\mathbf{G}) W(\mathbf{q}+\mathbf{G};\mathbf{k}',\mathbf{k}), \quad [7]$$

The publication costs of this article were defrayed in part by page charge payment. This article must therefore be hereby marked "*advertisement*" in accordance with 18 U.S.C. §1734 solely to indicate this fact.

Abbreviations: LDA, local density approximation; JT, Jahn–Teller.

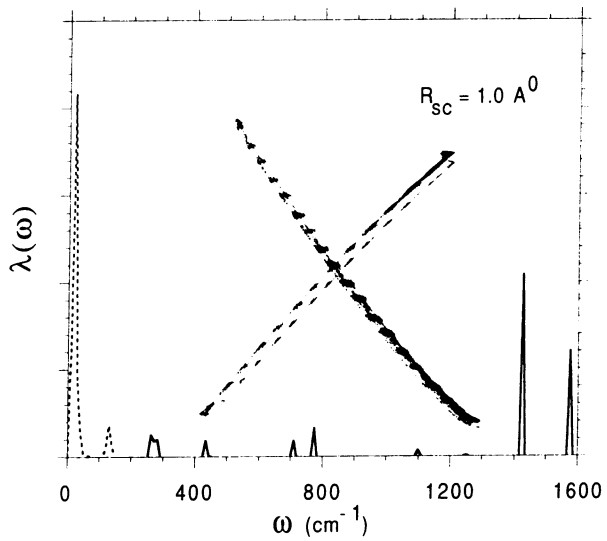

FIG. 1. Calculated values of $\lambda(\omega) = 2\alpha^2(\omega)F(\omega)/\omega$ using both Q and JT coupling; the dashed line is for $\lambda_Q(\omega)$, and the solid line is for $\lambda_{JT}(\omega)$. For $\omega < 200$ cm^{-1} all contributions are from Q, whereas for $\omega > 200$ cm^{-1} essentially all contributions are from JT. The maximum value of $\lambda(\omega)$ is 0.0669 cm.

where $W(\mathbf{q} + \mathbf{G}; \mathbf{k}',\mathbf{k}) = \Sigma_{m,n=1}^{3} A_m^*(\mathbf{k}')A_n(\mathbf{k})U_{mn}$ and $U_{mn} = \Sigma_i e^{-i\mathbf{k}'\cdot\mathbf{R}_i}\langle\psi_m(\mathbf{R}_i)|e^{i(\mathbf{q}+\mathbf{G})\cdot\mathbf{r}}|\psi_n(0)\rangle$. Here $\mathbf{q} = \mathbf{k}' - \mathbf{k} + \mathbf{G}$ is in the first Brillouin zone, $\mathbf{G}$ is a reciprocal lattice vector, $\mathbf{A}(\mathbf{k})$ is the electronic eigenvector of momentum $\mathbf{k}$, $\mathbf{R}_\alpha$ is the equilibrium position of the αth atom in the unit cell, ψ_m is a local Wannier wave function, and $\hat{V}_{ei}(\mathbf{q}) = 1/V_0 V_{ei}(\mathbf{q})$ (V_0 is the volume of a unit cell).

All quantities in Eqs. 4–7 were obtained directly from first-principles calculations except the screening length, R_{sc}. From Thomas–Fermi theory (17–19) an estimate is $R_{sc}^{TF} = \sqrt{E_f/6\pi e^2 n_e} = 0.63$ Å, where n_e is the conduction electron density and E_f is the Fermi energy for free electron gas. The proper value of R_{sc} for K_3C_{60} should be somewhat larger, perhaps 0.7–1.2 Å.

To calculate λ_Q, we used three p-like Gaussian functions on each C_{60} to describe approximate Wannier t_{1u} orbitals from the three electronic bands. A typical function is $\psi_x \propto x e^{-\alpha x^2 - \beta(y^2+z^2)}$, with $\alpha = 0.0397$ Å^{-2} and $\beta = 0.0550$ Å^{-2}. This treatment leads to analytic expressions for all integrals. We take the charge on each K as + electron and each C as −0.05 electron.

As indicated in Fig. 1, we find that $\lambda_Q(\omega)$ is negligible above 200 cm^{-1} and λ_Q has two peaks. One near $\omega_O \approx 20$–40 cm^{-1}, involves octahedral K plus C_{60} liberations; whereas the other at $\omega_T \approx 130$–150 cm^{-1} involves tetrahedral K.

Dynamic JT Coupling (H_{eph}^{JT}). Lannoo *et al.* (6, 7), Johnson *et al.* (8), and Varma *et al.* (9) suggested that JT coupling might play a role in the superconductivity, and Varma *et al.* (9) used modified neglect of differential overlap (MNDO) (20) calculations to estimate the couplings. We have repeated the estimates of Varma *et al.* (9) but using the vibrational modes from the GraFF (13) rather than from MNDO (20) (MNDO leads to frequencies ≈11% high). Letting g_m be the energy derivative with respect to displacement of m mode, we calculate (ref. 9 in parentheses): 0.19(0.1), 0.16(0.1), 0.26(0.2), 0.38(0.0), 0.26(0.6), 0.12(0.2), 1.77(1.8), and 1.49(1.2) for g_m of the eight H_g modes. This leads to (6–9)

$$\lambda_{JT,m} = \frac{5\,N(0)}{6\,M\omega_m^2}\,g_m^2, \qquad [8]$$

shown in Fig. 1. Thus $\lambda_{JT} = \Sigma_m \lambda_{JT,m} \sim \lambda_Q$ for $R_{sc} \approx 0.6$ to 1.0 Å.

Calculations of T_c

The Modified McMillan Equation. McMillan (21) and then Allen and Dynes (22) succeeded in developing a general formula for how the transition temperature T_c depends on the phonon density of states and the electron–phonon coupling matrix. Starting with

$$\alpha_{\mathbf{k}}^2(\omega)F_{\mathbf{k}}(\omega) = \frac{1}{(2\pi)^3}\sum_j \int \frac{d^2\mathbf{k}}{v_F}\,|M_{\mathbf{k}'\mathbf{k}j}|^2\delta(\omega - \Omega_{\mathbf{q}j})$$

$$\alpha^2(\omega)F(\omega) = \frac{1}{(2\pi)^3}\int \frac{d^2\mathbf{k}}{v_F}\,\alpha_{\mathbf{k}}^2(\omega)F_{\mathbf{k}}(\omega)\Big/\int \frac{d^2\mathbf{k}}{v_F} \qquad [9]$$

$$\lambda = \int \lambda(\omega)d\omega = 2\int \alpha^2(\omega)F(\omega)\,\frac{d\omega}{\omega}, \qquad [10]$$

where $v_F = \frac{1}{\hbar}\partial\varepsilon_k/\partial k_\perp$ is the average Fermi velocity ($k_\perp$ is perpendicular to the Fermi surface), and λ is the coupling constant. They found that (21, 22)

$$T_c = \frac{\Theta}{1.20}\exp\left[-\frac{1.04(1+\lambda)}{\lambda - \mu^* - 0.62\lambda\mu^*}\right], \qquad [11]$$

where various quantities are defined in Table 1.

Results

Now defined are all quantities required to calculate the T_c from Eq. 11. Table 2 has the calculated superconducting

Table 1. Definitions of quantities in Eq. 11

$\Theta = f_1 f_2 \omega_{log}$	$\mu^* = N(0)V_c/[1 + N(0)V_c \log(E_e/\omega_{ph})]$
$f_1 = \left[1 + \left(\frac{\lambda}{\Lambda_1}\right)^{3/2}\right]^{1/3}$	$f_2 = 1 + \frac{\left(\sqrt{\langle\omega^2\rangle}/\omega_{log} - 1\right)\lambda^2}{\lambda^2 + \Lambda_2^2}$
$\Lambda_1 = 2.46\,(1 + 3.8\mu^*)$	$\Lambda_2 = 1.82\,(1 + 6.3\mu^*)\left(\sqrt{\langle\omega^2\rangle}/\omega_{log}\right)$
$\omega_{log} = \exp\left[\frac{2}{\lambda}\int_0^\infty \frac{d\omega}{\omega}\,\alpha^2(\omega)F(\omega)\log\omega\right]$	$\langle\omega^2\rangle = \frac{2}{\lambda}\int_0^\infty d\omega\,\alpha^2(\omega)F(\omega)\omega$

E_e and ω_{ph} are the characteristic energy of conduction electron and phonon, respectively, and $V_c = \langle 4\pi e^2/(k^2 + q_{sc}^2)\rangle$ is averaged over the Fermi surface. We take $E_e = E_\omega = 0.6$ eV (the bandwidth) and $\omega_{ph} = \omega_{log}$.

Table 2. Superconducting properties for different values of R_{sc} (the only variable in the calculations)

R_{sc} (Å)	λ_Q/λ_{JT}	μ^*	λ	T_c (K)	ΔT_c (K)†	α_C‡	α_K‡
0.50	0.17	0.29	0.90	9.7	−6.4 (−3.6)	−0.10	−0.02
0.63	0.36	0.29	1.06	11.6	−8.7 (−5.8)	0.02	0.02
0.80	0.77	0.27	1.38	16.2	−9.9 (−5.3)	0.15	0.12
1.00	1.48	0.25	1.93	17.7	−5.8 (−0.5)	0.16	0.23
2.00	7.04	0.21	6.23	20.0	−0.1 (+3.2)	−0.01	0.44
Exp.				18§, 19.3¶	−7.2‖	0.30 (6)††	

Exp., experimental results.
†Change in T_c for pressure = 1 GPa = 10 kbar; in parentheses is the change assuming $N(0) = 11.5$.
‡α is the isotope exponent ($T_c \propto M^{-\alpha}$). α_C for $^{12}C \rightarrow {}^{13}C$ and α_K for $^{39}K \rightarrow {}^{41}K$.
§Ref. 1.
¶Ref. 3.
‖Refs. 23–25.
††Ref. 26.

properties for various values of R_{sc}. These calculations use the density of states $N(0) = 11.5$ from our tight-binding calculations. The susceptibility and critical field (23) suggest that $N(0) \approx 10$–15, whereas NMR measurement (24) gives $N(0) \sim 20$. An early photoemission experiment (25) reported that $N(0) = 1.9$, which may be low due to the surface sensitivity of these experiments.

We see that $R_{sc} = 0.8$–2.0 Å leads to $T_c = 16$–20 K, in good agreement with experiment (1–3). This does not prove the Q–JT mechanism because T_c depends sensitively upon $N(0)$, but neither experiment nor theory provides a precise value. The real test must be other properties.

Superconducting K_3C_{60} leads to an unusually large drop of T_c under external pressure (26), $\Delta T_c \approx -7.2$ K for $P = 1$ GPa. Using our force field, we calculated directly the equilibrium structure (allowing buckling of the buckyballs) and phonons for $P = 1$ GPa and recalculated $\lambda(\omega)$. Here we used the LDA results (27) that $N(0)$ decreases 20% under 1-GPa external pressure. The theory leads to $\Delta T_c = -6$ to -10 K for $R_{sc} =$ 0.5 to 1.0 Å.

A second significant test is the shift of T_c with isotope substitution. Experiments lead to $\alpha_C = 0.30 \pm 0.06$ for K_3C_{60} (28) and $\alpha_C = 0.37 \pm 0.05$ for Rb_3C_{60} (29) [an early report (30) of $\alpha_C = 1.4 \pm 0.5$ may be inaccurate]. We recalculated all phonon states and $\lambda(\omega)$ for both $^{12}C \rightarrow {}^{13}C$ and for $^{39}K \rightarrow {}^{41}K$. The resulting $\alpha_C = 0.15$ and 0.16 for $R_{sc} = 0.8$ and 1.0 Å are in reasonable agreement with experiment (28–30), but R_{sc} outside this range would lead to α_C in clear disagreement with experiment. A test here would be to measure α_K, which we predict to be 0.12–0.23.

Discussion

Our conclusion is that the superconductivity of K_3C_{60} is explained quite well by the Q–JT electron–phonon coupling mechanism including both H^Q_{eph} and H^{JT}_{eph} (with $R_{sc} \approx 0.8$ to 1.0 Å). To test whether either H^Q_{eph} or H^{JT}_{eph} is sufficient, we carried out the same calculations using only one coupling.

Table 3. Effects of not having both Q coupling and JT coupling

	Q coupling			JT coupling		
R_{sc} (Å)	δT_c†	ΔT_c‡	T_c	δT_c†	ΔT_c‡	T_c
0.50	NS	NS	NS	0.20	−0.73	1.52
0.63	0.00	NS	0.00	0.02	−0.01	0.02
0.80	0.00	−0.34	0.34	0.00	0.00	0.00
1.00	0.00	−2.26	2.50	0.00	0.00	0.00
2.00	0.00	−3.56	13.12	NS	NS	NS

All quantities are in the units of K. NS indicates not superconducting.
†δT_c is the change for T_c upon $^{12}C \rightarrow {}^{13}C$.
‡ΔT_c for 1 GPa pressure.

Table 3 shows that neither H^Q_{eph} nor H^{JT}_{eph} alone accounts for the superconducting properties of K_3C_{60}. With $R_{sc} = 1.0$ Å, H^Q_{eph} leads to $T_c = 2.5$ K, which drops for smaller R_{sc}. Larger values of R_{sc} with H^Q_{eph} alone lead to higher T_c values (e.g., 13 K for $R_{sc} = 2.0$ Å) but $\alpha_C \approx 0$, in disagreement with experiment (28–30). Including only JT with $R_{sc} = 0.5$ Å leads to $T_c = 1.5$ K (which goes to zero for higher R_{sc}) and a negative value of α_C, also in disagreement with experiment (28–30); these results for JT alone differ from ref. 9 because they used a smaller, fixed value of μ^*.

The conclusion here is that synergy between H^Q_{eph} and H^{JT}_{eph} leads to the special properties of buckyball superconductors. In the range $R_{sc} = 0.8$–1.0 Å, $\lambda_Q/\lambda_{JT} \approx 0.8$–1.5, so that both contributions are comparable. With only H^Q_{eph}, T_c drops substantially because λ decreases and ω_{log} becomes very small (decreasing Θ of Eq. 11). For only JT, λ decreases, whereas ω_{log} is very large, leading to a high μ^* and, hence, a large negative exponential term in Eq. 11 and a low T_c.

The JT coupling essential to the Q–JT mechanism is large for C_{60} because of the high symmetry. Other buckyballs (C_{70}, C_{76}) have much lower symmetry and generally do not have a degenerate ground state (first-order JT coupling) for the anion. Because eliminating JT drops T_c from ~16–18 K to ~0–3 K, we expect other buckyballs to have $T_c < 3$ K (potassium-intercalated graphite has $T_c = 0.8$ K). We do not yet have a band structure for Rb_3C_{60} to fit to Eq. 3; however, we did a Q–JT calculation, assuming $R_{sc} = 0.8$ Å, taking Fermi surface and μ^* the same as K_3C_{60} and estimating $N(0) = 1.2 \times 11.5$ [based on the result of an LDA calculation (27)]. Using the phonon states and optimal structure for Rb_3C_{60} from our force field (13) leads to $T_c \approx 23.5$ K for Rb_3C_{60}, as compared with $T_c = 16.2$ K for K_3C_{60} [experimental values (1–3) are 29 and 19 K, respectively].

Summarizing, we find that a combination of the charge and JT electron–phonon couplings are responsible for the superconductivity in K_3C_{60}. This explains T_c, ΔT_c(1 GPa), and α_C (and predicts α_K). More definitive tests of this Q–JT mechanism will be the prediction of T_c for various mixed alkali systems (2–5) where T_c ranges from 2.5 to 33 K. There are no variables left to our disposal; thus the force fields (and hence phonons) are determined, R_{sc} must be ~ 0.8–1.0 Å, and the quantities in μ^* are defined. The only remaining variables have to do with the electronic states [e.g., $N(0)$ and Fermi surface], which will emerge from LDA calculations.

We thank Drs. Y. Guo and N. Karasawa for discussions and help in calculating phonon eigenvectors and frequencies. This work was supported by National Science Foundation Grant CHE-91-00284 and by the Materials Simulation Center (California Institute of Technology) supported by Department of Energy (Advanced Industrial Concepts Division), Allied–Signal, Asahi Glass, Asahi Chemical, BP America, Chevron, and Xerox.

1. Hebard, A. F., Rosseinsky, M. J., Haddon, R. C., Murphy, D. W. & Glarum, S. H. (1991) *Nature (London)* **350,** 600–601.
2. Rosseinsky, M. J., Ramirez, A. P., Glarum, S. H., Murphy, D. W., Haddon, R. C., Hebard, A. F., Palstra, T. T. M., Kortan, A. R., Zahurak, S. M. & Makhija, A. V. (1991) *Phys. Rev. Lett.* **66,** 2830–2832.
3. Holczer, K., Klein, O., Huang, S.-M., Kaner, R. B., Fu, K.-J., Whetten, R. L. & Diederich, F. (1991) *Science* **252,** 1154–1157.
4. Tanigaki, K., Ebbesen, T. W., Saito, S., Mizuki, J., Tsai, J. S., Kubo, Y. & Kuroskima, S. (1991) *Nature (London)* **352,** 222–223.
5. Tanigaki, K., Hirosawa, I., Ebbesen, T. W., Mizuki, J., Shimakawa, Y., Kubo, Y., Tsai, J. S. & Kuroshima, S. (1991) *Nature (London)* **356,** 419–421.
6. Lannoo, M., Baraff, G. A., Schluter, M. & Tomanek, D. (1991) *Phys. Rev. B* **44,** 12106–12108.
7. Schluter, M., Lannoo, M., Needels, M., Baraff, G. A. & Tomanek, D. (1992) *Phys. Rev. Lett.* **68,** 526–529.
8. Johnson, K. H., McHenry, M. E. & Clougherty, D. P. (1991) *Physica C* **183,** 319–323.
9. Varma, C. M., Zaanen, J. & Raghavachari, K. (1991) *Science* **254,** 989–992.
10. Zhang, F. C., Ogata, M. & Rice, T. M. (1991) *Phys. Rev. Lett.* **67,** 3452–3455.
11. Chakravarty, S., Gelfand, M. P. & Kivelson, S. (1991) *Science* **254,** 970–974.
12. Baskaran, G. & Tosatti, E. (1991) *Curr. Sci. (India)* **61,** 33–39.
13. Guo, Y., Karasawa, N. & Goddard, W. A., III (1991) *Nature (London)* **351,** 464–467.
14. Stephens, P. W., Mihaly, L., Lee, P. L., Whetten, R. L. & Huang, S. M. (1991) *Nature (London)* **351,** 632–634.
15. Zhou, O., Vaughan, G. B. M., Zhu, Q., Fisher, J. E., Heiney, P. A., Coustel, N., McCauley, J. P. & Smith, A. B., III (1992) *Science* **255,** 833–835.
16. Erwin, S. C. & Pickett, W. E. (1991) *Science* **254,** 842–845.
17. Fermi, E. (1928) *Z. Phys.* **48,** 73–79.
18. Thomas, L. H. (1927) *Proc. Cambridge Philos. Soc.* **23,** 542–548.
19. Mahan, G. D. (1981) *Many-Particle Physics* (Plenum, New York), pp. 420–422.
20. Dewar, M. J. S. & Thiel, W. (1977) *J. Am. Chem. Soc.* **99,** 4899–4917.
21. McMillan, W. L. (1968) *Phys. Rev.* **167,** 331–344.
22. Allen, P. B. & Dynes, R. C. (1975) *Phys. Rev. B* **12,** 905–922.
23. Ramirez, A. P., Rosseinsky, M. J., Murphy, D. W., Fleming, R. M. & Haddon, R. C. (1992) *Bull. Am. Phys. Soc.* **37,** 714 (abstr.).
24. Tycko, R., Dabbagh, G., Rosseinsky, M. J., Murphy, D. W. & Fleming, R. M. (1991) *Science* **253,** 884–886.
25. Chen, C. T., Tjeng, L. H., Rodolf, P., Meigs, G., Rowe, J. E., Chen, J., McCauley, J. P., Smith, A. B., McGhie, A. R., Romanow, W. J. & Plummer, E. W. (1991) *Nature (London)* **352,** 603–605.
26. Sparn, G., Thompson, J. D., Huang, S.-M., Kaner, R. B., Diederich, F., Whetten, R. L., Gruner, G. & Holczer, K. (1991) *Science* **252,** 1829–1831.
27. Oshiyama, A. & Saito, S. (1992) *Solid State Commun.* **82,** 41–45.
28. Chen, C.-C. & Lieber, C. M. (1992) *J. Am. Chem. Soc.* **114,** 3141–3142.
29. Ramirez, A. P., Kortan, A. R., Rosseinsky, M. J., Duclos, S. J., Mujsce, A. M., Haddon, R. C., Murphy, D. W., Makhija, A. V., Zahurak, S. M. & Lynos, K. B. (1992) *Phys. Rev. Lett.* **68,** 1058–1060.
30. Ebbesen, T. W., Tsai, J. S., Tanigtaki, K., Tabuchi, J. & Shimakawa, Y. (1992) *Nature (London)* **355,** 620–622.